ELSEVIER

Thermochimica Acta 249 (1995) 325–333

thermochimica acta

# Thermal decomposition of $Bi_2STe_2$ tetradymite

I.L. Botto[a,*], A.M. Ramis[a], I.B. Schalamuk[b], M.A. Sanchez[c]

[a]*Química Inorgánica (QUINOR), Facultad de Ciencias Exactas, Universidad Nacional de La Plata, C. Correo 962, 1900 La Plata, Argentina*

[b]*Centro de Investigación de Recursos Minerales (INREMI), Facultad de Ciencias Naturales, Universidad Nacional de La Plata, 1900 La Plata, Argentina*

[c]*Comisión de Investigaciones Cientificas PBA and CINDECA, 1900 La Plata, Argentina*

Received 22 October 1993; accepted 1 May 1994

**Abstract**

The oxidative thermal decomposition of natural tetradymite ($Bi_2STe_2$) has been studied by thermal techniques and by X-ray diffraction, infrared spectroscopy and scanning electron microscopy. Oxidation occurs exothermically at comparatively low temperatures, whereas desulfatization takes place endothermically at higher temperatures. A scheme for the overall reaction is proposed. The exothermic process occurs at lower temperature for material of smaller particle size.

*Keywords:* Coupled technique; IRS; SEM; Sulphide; Ternary system; Tetradymite; XRD

## 1. Introduction

The oxidation of common sulfides such as pyrite, chalcopyrite, galena, cinnabar and molybdenite has been extensively studied by thermal analysis. Reaction schemes for these processes have been also proposed [1–6].

The effects of different experimental variables, such as atmospheric conditions, heating rate or mechanical activation, have been investigated because of the technological importance of this type of process as a preliminary operation in pyrometallurgy [7–10]. However, the oxidative thermal behavior of complex

* Corresponding author.


*SSDI* 0040-6031(94)01897-P

sulfides which contain Te, Bi, As and Sb, as well as Ag, Cu, Zn, Pb and Au in some cases [11], is less well known. These species are usually present, although in small proportions, in sulfide deposits and in other types of natural sources.

This paper reports the thermal decomposition of natural $Bi_2STe_2$ (tetradymite) isolated from the pegmatitic formation of Cerro Blanco, Tanti, province of Cordoba, Argentina. This mineral has been found principally associated with quartz, feldspar and micas in addition to pyrite, chalcopyrite and their oxidation products [12].

To analyze the course of the oxidative process, a study was carried out by simultaneous thermogravimetry–differential thermal analysis (DTA–TG), with the aid of X-ray diffraction (XRD), infrared spectroscopy (IRS) and scanning electron microscopy (SEM). The effect of the particle size of the sample has also been considered.

## 2. Experimental

The material used in the study was selected by hand picking, and its purity was checked by XRD, electron probe microanalysis (EPMA) and standard chemical analysis. In general, the samples were revealed as being single phases by XRD. However, the presence of small inclusions of quartz and other impurities could be also observed by SEM in some samples. The analysis by SEM was carried out on a Philips 505 with an EDAX 9100 instrument and an energy dispersive detector. For the quantitative EPMA, $BiO_2O_3$, $TeO_2$ and S (all analytical-grade reagents) were used as reference materials. The composition of 59.38% Bi, 36.12% Te and 4.50% S is in good agreement with the theoretical values for $Bi_2STe_2$ (59.27% Bi, 36.17% Te and 4.55% S), although the compositional limits of tetradymite have been shown to be $Bi_2STe_2$–$Bi_2S_{1.3}Te_{1.7}$ [13].

The TG–DTA experiments were carried out on a Rigaku thermoanalyzer (type YLDG/CN 8002 L2) using a chromel–alumel thermocouple and a constant air flow of 0.40 l $min^{-1}$. About 20 mg portions of specimen were weighed. The heating rate was 10°C $min^{-1}$, and $\alpha$-$Al_2O_3$ was used as DTA standard. The temperature was raised to 700°C. The measurements were performed at two different particle sizes: $\approx 2$ mm and $\approx 125$ μm (standard sieves Nos. 10 and 120 respectively). Additional thermal studies were carried out up to 950°C in a programmed temperature furnace, in an air atmosphere, using an alumina crucible. The heated samples were investigated by XRD with a Philips PW 1714 diffractometer (Cu K$\alpha$ radiation, Ni filter) diffractometer. NaCl was used as an external standard in the quantitative analysis. The program PIRUM developed by Werner [14] was used to refine the cell parameters.

The IR spectroscopic analyses, as usually used to identify the intermediates of sulfide oxidation [15–17], were carried out on a Perkin-Elmer 580-B spectrophotometer using a KBr pellet technique.

## 3. Results and discussion

Typical TG and DTA curves are shown in Fig. 1, where the effect of the particle size can be observed. Exothermic oxidation reactions prevail in the low temperature region, with the formation of sulfate, whereas desulfatization is an endothermic process that occurs at higher temperatures. This behavior is similar to that observed for other, related compounds [1,8,15].

Fig. 2 shows the IR spectra of tetradymite samples (particle size 125 μm) at different stages of decomposition. Additional spectra are included for comparative purposes. Fig. 2(a) corresponds to the natural sample (without thermal treatment). Only a weak band is observed at 335 $cm^{-1}$, which is assigned to the Bi–S stretching [16]. The spectrum of the mineral species heated up to 300°C (Fig. 2(b)), which is X-ray amorphous, reveals the presence of weak bands at 1100 and 650 $cm^{-1}$, which correspond to the incipient formation of sulfate [18]. It is well known that for the $SO_4^{2-}$ ion, which belongs to the $T_d$ symmetry group, the IR bands are located at 1105 $cm^{-1}$ ($\nu_3$), 983 $cm^{-1}$ ($\nu_1$), 611 $cm^{-1}$ ($\nu_4$) and 1450 $cm^{-1}$ ($\nu_2$) [18]. Fig. 2(c) shows the $Bi_2(SO_4)_3$ spectrum as a reference. The $\nu_1$ and $\nu_3$ symmetric and antisymmetric stretchings have been assigned, together with the similar bending modes of the tetrahedral sulfate ($\nu_2$ and $\nu_4$ respectively). The spectrum of the sample heated up to 400°C is shown in Fig. 2(d). The similarity between the spectra shown in Figs. 2(c) and 2(d) is clear. However, the asymmetry of the band centered at 648 $cm^{-1}$ (with a shoulder at $\approx 670$ $cm^{-1}$) and the weak bands in the lower region of

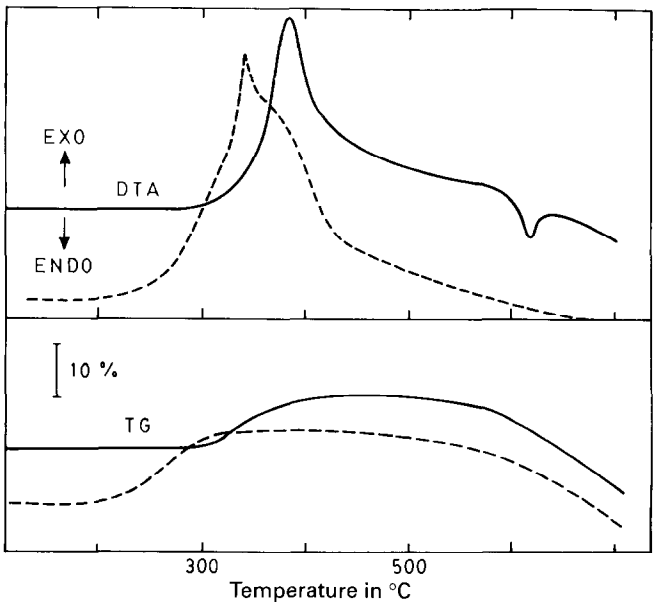


Fig. 1. TG–DTA curves of tetradymite: particle size ≈ 2 mm (solid line); particle size ≈ 125 μm (broken line).

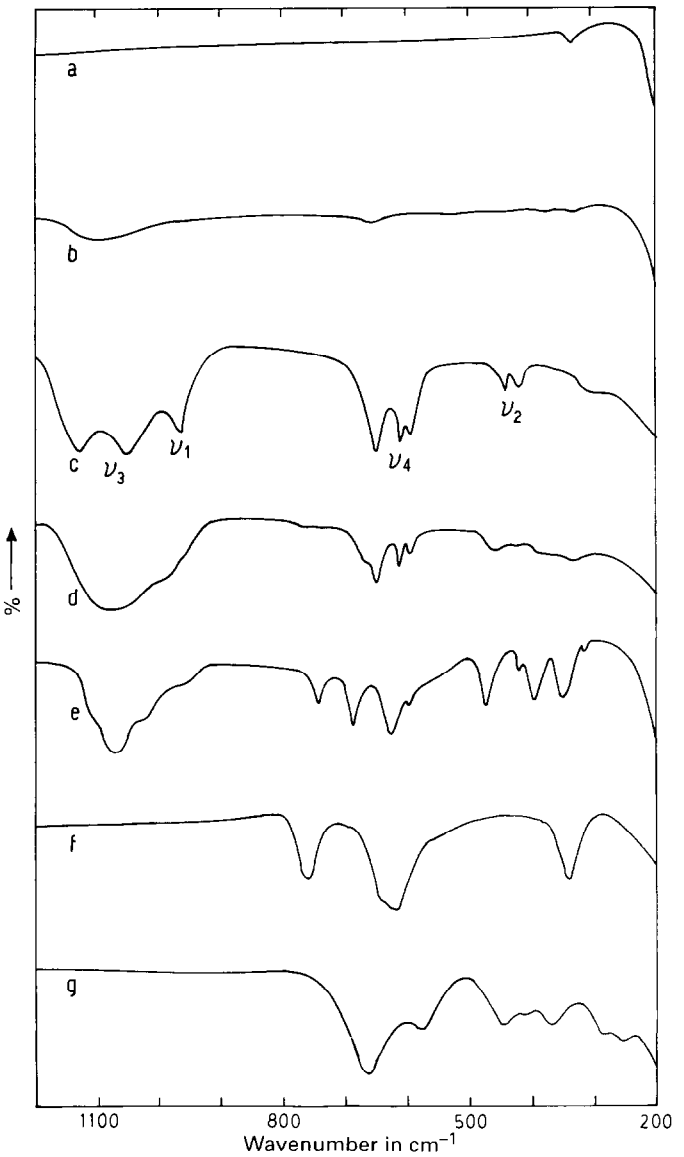


Fig. 2. Comparative IR spectra: (a) tetradymite without thermal treatment, (b) sample heated at 300°C, (c) $Bi_2(SO_4)_3$, (d) sample heated at 400°C, (e) sample heated at 500°C, (f) $TeO_2$, (g) sample heated at 950°C.

the spectrum suggest the presence of another oxidic phase. These bands could be attributed to some $Bi_2O_3$ polymorphic phase [19]. At 400°C the sample is still amorphous to X-rays. The presence of the sulfate species becomes more evident in the spectrum 2(e), which corresponds to tetradymite heated to 500°C.

In this spectrum, some other bands below 800 $cm^{-1}$ can be clearly assigned to $TeO_2$ (paratellurite), the spectrum of which is shown in Fig. 2(f) for reference. Likewise, the band located at 680 $cm^{-1}$ can be probably assigned to the $BiO^+$ bismuthyl species, as it has been reported that $Bi_2(SO_4)_3$ is converted to $(BiO)_2SO_4$ at 400°C [20].

In relation to the thermal behavior of tellurium oxide, it is interesting to note that the thermal decomposition of orthotelluric acid in air has already been studied and the final product is tellurium dioxide (paratellurite) [21–24]. This product is obtained in the range 480–500°C, and it melts to yield amorphous $TeO_2$ between 550 and 600°C. Its sublimation occurs in the region of 700°C [15,23]. The weight loss of $\approx 10\%$ in the mineral sample heated at 700°C (which reaches $\approx 17\%$ at 800°C) suggests this type of process. The spectra remain practically unchanged from these temperatures up to 950°C. The spectrum of the sample heated at this temperature may be observed in Fig. 2(g), and is similar to that of $\delta$-$Bi_2O_3$ with a cubic phase related to the fluorite structure.

The scanning electron micrographs of the original tetradymite, and those of samples obtained at different stages of decomposition, are shown in Fig. 3. A comparison between the micrographs of unreacted particles of tetradymite (size $\approx 1$ mm, Fig. 3(a)) and of particles heated at 400°C reveals that, in general, the latter have undergone significant reaction, especially at the rim (Fig. 3(b)). However, the greatest oxidation occurs between 450 and 500°C (Fig. 3(c)), where there is a clear alteration of the surface. Fig. 3(d) corresponds to a sample heated in similar conditions but with higher particle size ( $\approx 2$ mm). Small particles have a greater interfacial area available for oxidation and react faster than the larger ones. Evidently the oxidation process takes place via oxygen diffusion. Likewise, the distance required for the diffusion of oxygen into the particles is lower for the smaller particles. This leads to more efficient oxidation. The product layer on the surface evidently contributes to the inhibition of the diffusion process. Finally, Figs. 3(e) and 3(f) show the morphology of tetradymite heated to 800 and 950°C respectively.

The IR spectra suggest that the formation of $TeO_2$ starts at 400°C, and it is clearly observed at 500°C, in agreement with literature data. Although this oxide sublimes at temperatures above 600°C, the Te:Bi ratio is 18.5:81.5 at 800°C, and the presence of S is not detected. These data, which remain unchanged up to 950°C, are in agreement with the theoretical values for the formal "$Bi_8Te_3O_{18}$" phase (in which the Te:Bi ratio is 18.63:81.37).

In the study of phases belonging to the $Bi_2O_3$–$TeO_2$ system [25], the formation of the cubic (fcc) $Bi_{1-x}Te_xO_{(1.5+x/2)}$ solid solution phase has been detected up to $x \approx 0.4$. The presence of a phase of composition $Bi_{0.723}Te_{0.273}O_{1.6365}$ can be inferred from the electron microprobe results. This assumption can be corroborated from the $a = 0.559(1)$nm cubic cell parameter calculated from XRD data and with the aid of the plot that shows the variation of the cubic lattice parameter of the $Bi_{1-x}Te_xO_{(1.5+x/2)}$ oxidic phase (derived from $\delta$-$Bi_2O_3$) with $x$ [25]. The melting point is near 950°C for this composition [25], but the quenched sample has a similar structure to the fcc phase. Thus, the micrograph 3(f) reveals a significant degree of melting.

Hence a scheme of the oxidation reaction (Scheme 1) can be proposed

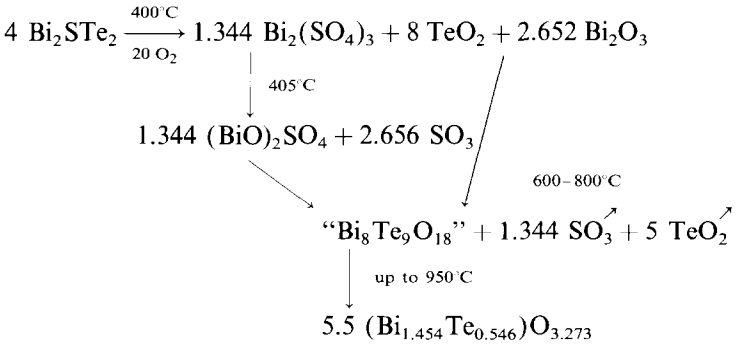


Scheme 1. The oxidation reaction.

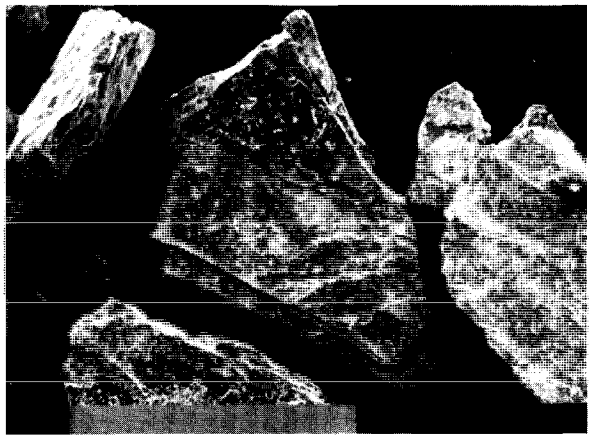

(a)

(b)

Fig. 3(a, b)

(c)

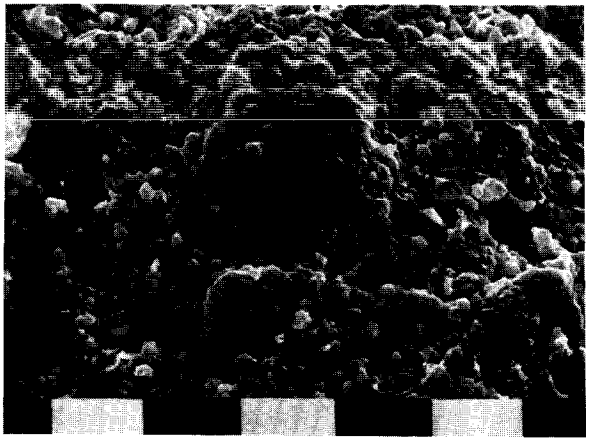

(d)

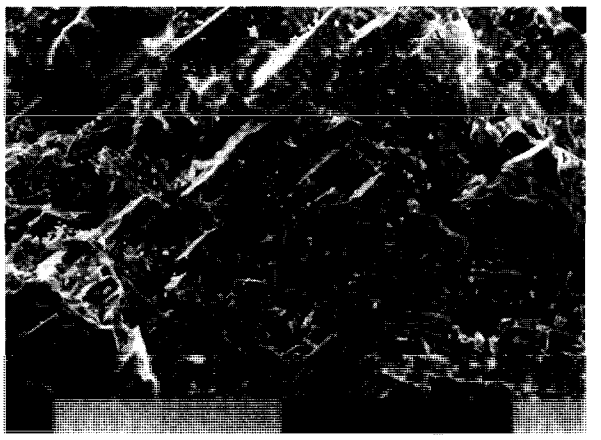

(e)

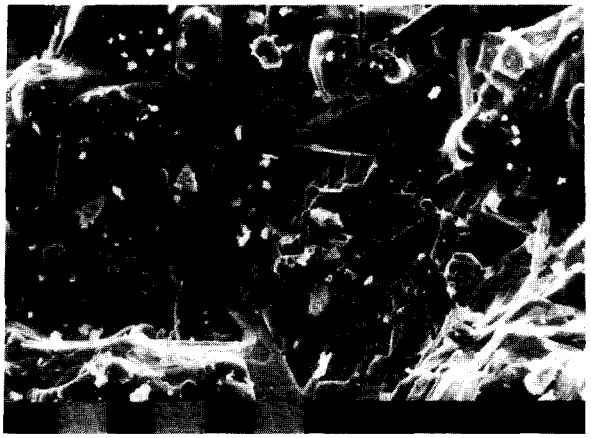

(f)

Fig. 3. Scanning electron micrographs of: (a) tetradymite without thermal treatment (particle size ≈1 mm, (original magnification × 63, scale bar 1 mm), (b) sample heated at 400°C (original magnification × 2000, scale bar 10 μm), (c) sample heated at 500°C (original magnification × 2000, scale bar 10 μm), (d) similar heating conditions, particle size ≈2 mm (original magnification × 2000, scale bar 10 μm), (e) sample heated at 800°C (original magnification × 1000, scale bar 10 μm), (f) sample heated at 950°C (original magnification × 500, scale bar 100 μm).

## 4. Conclusions

The oxidative decomposition of tetradymite is a very complex process that leads to the formation of bismuth sulfate and bismuthyl sulfate as intermediates. Likewise, the $TeO_2$ formed at ≈400°C reacts partially with the $Bi_2O_3$ obtained by decomposition of the sulfate. A stable solid solution of composition $(Bi_{1.454}Te_{0.546})O_{3.273}$ structurally related to cubic fluorite is clearly observed. Finally, the process is affected by grinding. Thus, the exothermic oxidative reaction occurs at a lower temperature as the particle size decreases.

## Acknowledgments

This work was supported by CONICET and CICPBA, Argentina.

## References

[1] D.N. Todor, Thermal Analysis of Minerals, Abacus Press, Tunbridge Wells, 1976.
[2] G. Bayer and H.G. Wiedemann, Thermochim. Acta, 198 (1992) 303.
[3] P. Balaz, H.J. Huhn and H. Heegn, Thermochim. Acta, 194 (1992) 189.
[4] S.A.A. Jayaweera, J.H. Moss and A. Wearmouth, Thermochim. Acta, 152 (1989) 237.
[5] Y. Shigegaki, S.K. Basu, M. Wakihara and M. Taniguchi, J. Therm. Anal., 34 (1988) 1427.

[6] K. Laajalehto, R. St. C. Smart, J. Ralston and E. Suoninen, Appl. Surf. Sci., 64 (1993) 29.
[7] P. Balaz, E. Post and Z. Bastl, Thermochim. Acta, 200 (1992) 371.
[8] K. Trakova, P. Balaz and T.A. Korneva, J. Therm. Anal., 34 (1988) 1031.
[9] J.G. Dunn, G.C. De and B.D. O'Connor, Thermochim. Acta, 145 (1989) 115.
[10] J.G. Dunn, G.C. De and B.D. O'Connor, Thermochim. Acta, 155 (1989) 135.
[11] E. Makovicky, Neues. Jb. Miner. Abh., 160 (1989) 369.
[12] S. Rivas, Rev. Min., 29 (1969) 47.
[13] P. Bayliss, Am. Mineral., 76 (1991) 257.
[14] P.E. Werner, Ark. Kemi, 31 (1969) 513.
[15] I.L. Botto and I.B. Schalamuk, Thermochim. Acta, 128 (1988) 311.
[16] J.G. Dunn, W. Gong and D. Shi, Thermochim. Acta, 208 (1992) 293.
[17] J.G. Dunn, W. Gong and D. Shi, Thermochim. Acta, 215 (1993) 247.
[18] H. Siebert, Anwendungen der Schwingungsspektroskopie der Anorganischen Chemie, Springer-Verlag, Berlin, 1966.
[19] N.T. McDevitt and W.L. Baun, Spectrochim. Acta, 20 (1964) 799.
[20] C. Duval, Inorganic Thermogravimetric Analysis, 2nd edn., Elsevier, 1963.
[21] J. Rosicky, J. Loub and J. Pavel, Z. Anorg. Allg. Chem., 334 (1965) 312.
[22] J. Fabry, J. Loub and L. Feltl, J. Therm. Anal., 24 (1982) 95.
[23] I.L. Botto, J. Less-Common Met., 128 (1987) 47.
[24] J. Loub, Collect. Czech. Chem. Commun., 58 (1993) 1717.
[25] T. Kikuchi, Y. Kitami, M. Yokoyama and H. Sakai, J. Mater. Sci., 24 (1989) 4275.